Supramolecular Alloys from Fluorinated Hybrid Tri^{4}Di^6 Imine Cages

Tom Kunde[+],[a] Tobias Pausch[+],[a] and Bernd M. Schmidt*[a]

Abstract: To create innovative materials, efficient control and engineering of pore sizes and their characteristics, crystallinity and stability is required. Eight hybrid Tri^{4}Di^6 imine cages with a tunable degree of fluorination and one fully fluorinated Tri^{4}Di^6 imine cage are investigated. Although the fluorinated and the non-fluorinated building blocks used herein differ vastly in reactivity, it was possible to gain control over the outcome of the self-assembly process, by carefully controlling the feed ratio. This represents the first hybrid material based on fluorinated/hydrogenated porous organic cages (POCs). These cages with unlimited miscibility in the solid state were obtained as highly crystalline samples after recrystallization and even showed retention of the crystal lattice, forming alloys. All mixtures and the fully fluorinated Tri^{4}Di^6 imine cage were analyzed by MALDI-MS, single-crystal XRD, powder XRD and in regard to thermal stability (TGA).

Nature efficiently uses the principles of non-covalent self-assembly together with self-sorting phenomena to generate complex, functional architectures from several different and often complex building blocks bearing function. In an abiological context, the design of porous materials, suitable for gas adsorption applications, requires precise control over the interior and exterior pore size, accessibility and the stability of the material itself.[1] A large range of materials, containing a high amount of fluorine atoms, have in the past been attributed with increased thermal stability, higher crystallinity and higher gas uptake compared to their non-fluorinated counterparts.[2–5] The group of Miljanić was able to capture fluorinated anesthetics inside a porous crystal, consisting of extensively fluorinated aromatic molecules.[6a,b] The beneficial effect of fluorine substitution does even further extend to increased crystallinity, not only in the crystal lattice of small molecules, but also in COFs.[5,7] Dynamic covalent bond formation, often employing amine and aldehyde building blocks for self-correcting imine formation, generates dynamic cage-type compounds with various properties up to complex multi-component libraries.[8] Porous organic cages (POCs), as an emerging class of porous materials, have been extensively studied throughout the last decade.[9a,c,10e–g] Significant contributions include control of pore size,[9b,e,10b] cage and pore geometry,[9f,10d] guest binding behavior[10g] and engineering of the overall crystal packing,[9f,10f] demonstrating a great degree of control over the material properties.[9,10] Only few articles focus on the role of fluorine in dynamic imine chemistry and as the possibility to influence porosity and guest-binding behavior of POCs.[10b,11] Recently, we were able to demonstrate the beneficial effect of fluorine substitution[12] towards gas adsorption of POCs.[13]

Herein, we investigate the synthesis of hybrid-POCs containing non-fluorinated and fluorinated building blocks, resulting in a complex dynamic material library. We examine the different reactivities of the two isostructural ditopic aldehydes[8j] and their influence on the outcome of dynamic Tri^{4}Di^6 imine condensations. The effect of fluorine substitution on the thermal stability and crystallinity of these novel hybrid materials is analyzed to evaluate the result of our library approach. In the high-throughput study of Cooper and co-workers, the formation of a Tri^{4}Di^6 imine cage by reaction of four 1,3,5-tris(2-aminomethyl)-2,4,6-triethyl-benzene (**A**) units with six terephthalaldehyde molecules (**TA**) was reported.[9d] We chose this motif to subsequently exchange the six non-fluorinated **TA** building blocks for tetrafluoroterephthalaldehyde (**TFTA**), allowing us to precisely monitor the influence of fluorinated subunits in relation to cage properties (solid state self-assembly and thermal stability). The large difference in electron density and overall quadrupolar moment is envisioned to have a significant effect on the cavity of the resulting imine cages. We present a series of eight partially fluorinated imine cages, as well as a fully fluorinated Tri^{4}Di^6 imine cage using building blocks with a large difference in reactivity for the first time.

Previous studies utilized chiral self-sorting[10c] or structurally different building blocks to desymmetrize POCs by imine condensation to create amorphous materials.[14] Along with increasing disorder within the material, this approach allows us to generate a crystalline supramolecular alloy after recrystallisation of the hybrid cage mixtures, freely composed of highly fluorinated and non-fluorinated POCs.[15]

[a] *T. Kunde,[+] T. Pausch,[+] Dr. B. M. Schmidt*
Institut für Organische Chemie und Makromolekulare Chemie
Heinrich-Heine-Universität Düsseldorf
Universitätsstraße 1, 40225 Düsseldorf (Germany)
E-mail: Bernd.Schmidt@hhu.de
Homepage: http://www.bmschmidtlab.de

[+] *These authors contributed equally to this work.*

Supporting information for this article is available on the WWW under https://doi.org/10.1002/chem.202100891

© 2021 The Authors. Published by Wiley-VCH GmbH. This is an open access article under the terms of the Creative Commons Attribution Non-Commercial License, which permits use, distribution and reproduction in any medium, provided the original work is properly cited and is not used for commercial purposes.

Five equivalents of amine **A** (slight excess) were reacted with varying ratios of **TA** and **TFTA** at room temperature in either methanol or chloroform with an amine concentration of 4 mmol/L. As a systematic nomenclature for these mixed cages we use $\mathbf{A_4H_XF_{(6-X)}}$ herein, where X is the number of incorporated **TA** molecules and the number following the letter **F** represents the number of **TFTA** moieties per cage molecule (Figure 1). After a period of 2 days, we could isolate a colorless solid directly from the reaction mixture by filtration. Analysis by ^{1}H, ^{19}F NMR and DOSY experiments after redissolving the solids revealed the successful synthesis of a narrow distribution of hybrid cage species around the targeted composition. All cage compounds within the mixture following the composition $\mathbf{A_4H_XF_{(6-X)}}$, are expected to be of similar size and indeed show comparable diffusion coefficients around $D = 4.5*10^{-10}\ m^2 s^{-1}$ corresponding to a solvodynamic radius of 0.90 nm in solution (Table S1). A statistical distribution of the mixed cages $\mathbf{A_4H_5F_1}$, $\mathbf{A_4H_4F_2}$ and $\mathbf{A_4H_3F_3}$ alongside $\mathbf{A_4H_6}$ is also confirmed by MALDI-MS analysis of the precipitate (Figures S59-S68). According to the general procedure, to our delight, all anticipated hybrid cage mixtures with varying fluorine content can be accessed and were characterized as obtained from the reaction mixture comprehensively by using MALDI-MS, NMR and powder XRD (Figures S39 and S46-S68). Directly corresponding to the feed ratio of **TA** and **TFTA**, a narrow gaussian-like distribution around the targeted composition demonstrates very good control over the outcome of the cage formation even after recrystallization (Figure 2).

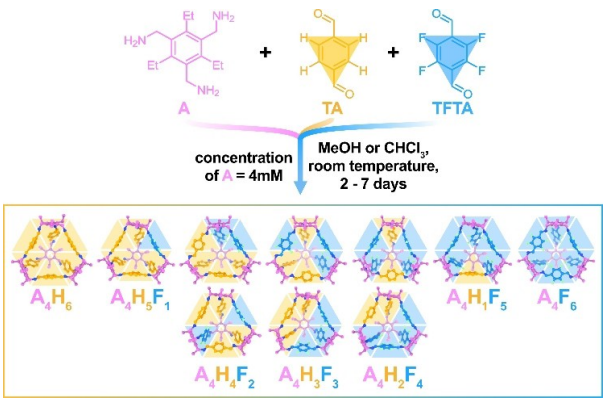

Figure 1. Synthetic scheme of the reaction of amine **A** with **TA** and fluorinated **TFTA**, in different feed ratios, targeting the hybrid cages $\mathbf{A_4H_XF_{(6-X)}}$; the hexagons indicate the corresponding compositions of the hybrid cages throughout the manuscript.

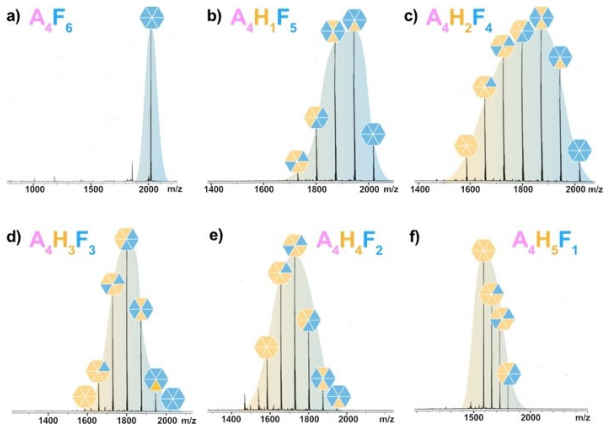

Figure 2. MALDI-MS spectra of the recrystallized cage alloys a) $\mathbf{A_4F_6}$, b) $\mathbf{A_4H_1F_5}$, c) $\mathbf{A_4H_2F_4}$, d) $\mathbf{A_4H_3F_3}$, e) $\mathbf{A_4H_4F_2}$ and mixture f) $\mathbf{A_4H_5F_1}$ obtained using different feed ratios of **TA** and **TFTA** with 5 equivalents of amine **A**, inlays each indicate the targeted composition. Using a slight excess of amine **A**, yields are significantly improved.[9d] For the MALDI-MS spectra of all mixtures isolated directly from the reaction by either filtration or evaporation of the solvent at ambient temperatures, see Figures S59-S68.

Considering **TFTA** bears four highly electronegative substituents, we were intrigued to examine the differences in reactivity compared to **TA**, since the synthesis of imine cages is often accompanied by precipitation of the product from the reaction solvent. In those cases, the time until precipitation occurs, can serve as an indicator for reactivity. To study these differences, chloroform was chosen as solvent. In our experience, possible oligomeric side products are solubilized efficiently in chloroform, facilitating error correction of dynamic imine condensation reactions. Under these given conditions, pure $\mathbf{A_4H_6}$ and $\mathbf{A_4H_5F_1}$ mixtures start to precipitate after 24 h, whereas all cage mixtures with a **TFTA** count >1 start precipitating almost immediately (as indicated by NMR experiments, Figure S1-S2). This underlines the anticipated high reactivity of the **TFTA** molecules and hence, shorter reaction times. But one has to consider, that **TFTA** containing cage products are also often less soluble in comparison to non-fluorinated congeners, from our observations. To further investigate the different reactivities, we conducted kinetic NMR experiments and DFT calculations (Figures S1-S4 and S17). The two approaches to generate essentially all $\mathbf{A_4H_XF_{(6-X)}}$ species are: a) by mixing the pure $\mathbf{A_4F_6}$ and $\mathbf{A_4H_6}$ cages in the corresponding ratios to generate a distribution of mixed cage compounds in hot chloroform over prolonged time (Figures S6 and S7) or b), by mixing **TFTA** and **TA** with the amine **A** in ratios corresponding to the targeted $\mathbf{A_4H_XF_{(6-X)}}$ composition. The latter approach is clearly faster since the reaction times are only 2–3 days instead of several weeks needed for the former system to reach its equilibrium state.

Immediately after mixing, the consumption of **TFTA** can be observed. Fast formation of precipitate (potentially oligomeric species with high fluorine content) can be noted, without new imine signals in ^{1}H NMR being observed. **TFTA** is consumed completely, before the majority of **TA** reacted. The oligomeric species containing **TFTA** appear to act as a reservoir and are not removed from the system completely (Figures S1 and S2). Redissolved fragments react then with the less reactive **TA** building blocks in a dynamic equilibrium, resulting in the observed mixtures, an important addition to the recent investigation on hydrogenated and deuterated POCs.[16]

As anticipated, the decomposition temperatures are increasing with higher fluorine content. The onset temperature of $\mathbf{A_4H_6}$, 266 °C could be increased to 313 °C for $\mathbf{A_4F_6}$. Each subsequent substitution of **TA** *versus* **TFTA** increases the decomposition onset by roughly 5 °C (Figure 3e). This is in perfect agreement with the influence of fluorine substitution on porous organic materials.[2d]

© 2021 The Authors. Published by Wiley-VCH GmbH

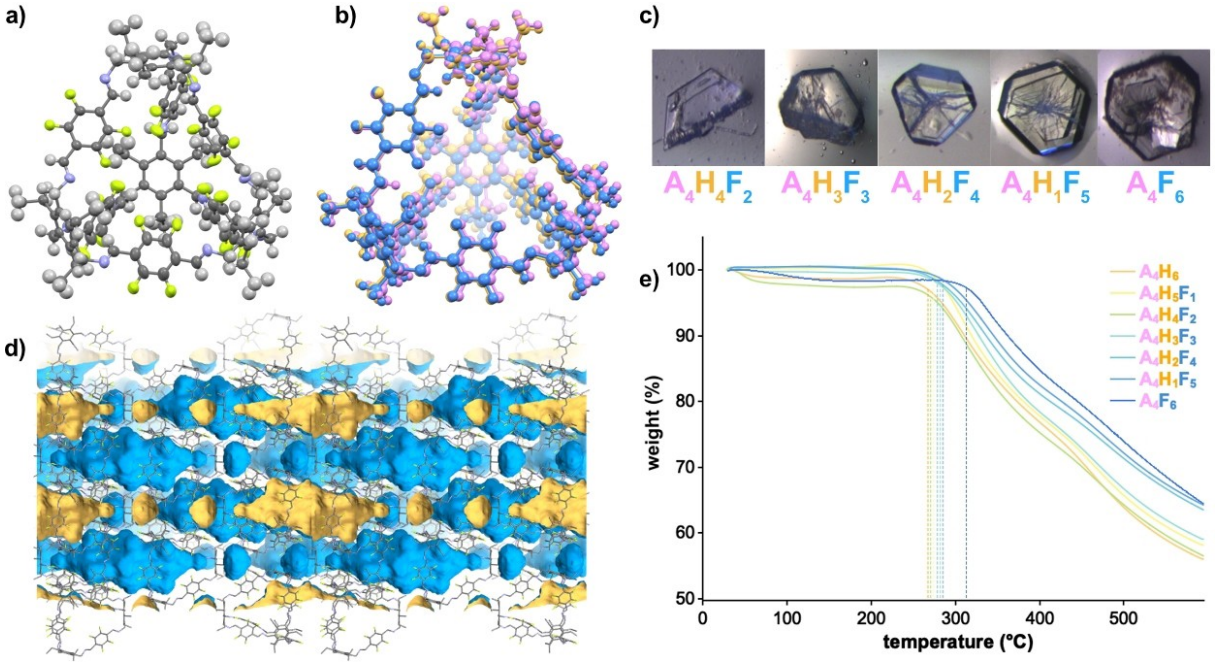

Figure 3. a) Structure of $\mathbf{A_4H_2F_4}$ obtained from single-crystal XRD data; the structure was measured at 100 K and solved in the rhombohedral *R-3* with R_{Int} = 0.1182, R_1 = 0.0931 and wR_2 = 0.3157, the fluorine content is estimated to be 48 percent for both crystallographically unequal fluorobenzenes within the structure (the variance is the highest for $\mathbf{A_4H_2F_4}$ because of a low resolution and framework disorder, see the Supporting Information); solvents are omitted for clarity. b) Overlay of the crystal structures for $\mathbf{A_4F_6}$ (blue), $\mathbf{A_4H_1F_5}$ (pink) and $\mathbf{A_4H_2F_4}$ (orange). c) Microscopic photographs taken of single-crystals before XRD measurements (approx. 0.2–0.3 mm). d) Solvent accessible surface area without solvents for a molecular probe with 1.2 Å radius (outer surface area = blue, inner surface = orange) within the crystal lattice. e) Thermogravimetric analyses of all hybrid cage mixtures; the dotted lines indicate the onset temperature of decomposition (Table S2).

We were able to obtain single-crystals (Figure 3a) of all targeted imine cage compounds and obtained structural data for pure $\mathbf{A_4F_6}$ and $\mathbf{A_4H_1F_5}$, $\mathbf{A_4H_2F_4}$, $\mathbf{A_4H_4F_2}$ alloys.[17] The hybrid cages crystallize in regular rhombohedral shapes (Figure 3c). To our surprise, the single-crystals also did not consist of one cage isomer but exhibited the same gaussian distribution of hybrid cages, within the crystal lattice (Figures S61-S67). All hybrid cage alloys crystallize in the highly symmetric rhombohedral space group *R-3*, with one whole and a third molecule **A** and two *para*-substituted building blocks in the asymmetric unit. Due to their large size and voids containing ordered and disordered solvent molecules within the lattice, refinement was carried out as described for each crystal (see Supporting Information, page S29 ff.). The **TFTA** and **TA** motifs can be exchanged freely in the crystal lattice at the two available, crystallographically independent positions and are furthermore moved by the representative symmetry operations. The average fluorine content was estimated from the diffraction data and compared to MALDI-MS data of the single-crystals, showing excellent agreement. In the solid state, two adjacent cages pack window-to window generating a pore of roughly 18 Å length, as depicted (Figure 3d). Close π-π-stacking in a distance of about 3.5 Å connects neighboring cages, whereas stacking with former amine building block **A** is hampered by the bulky ethyl groups, leading to centroid-to-centroid distances of around 4.5 Å. These results suggest a) the influence of fluorinated building blocks on the crystallinity, as only the non-fluorinated imine cage could not be crystallized and b) an interchangeability of **TFTA** and **TA** both in the parent cage (multivariate)[18] and in the crystal lattice of these Tri^4Di^6 imine cages (Figure 3b), making them indeed tunable supramolecular alloy materials in the solid state. For the crystal of $\mathbf{A_4H_2F_4}$, this would essentially result in a septenary crystal not counting isomers, which would even imply a denary cocrystal (see Figure 2c).

We successfully synthesized and characterized a family of dynamic Tri^4Di^6 imine cages, $\mathbf{A_4H_XF_{(6-X)}}$, containing highly fluorinated building blocks. To the best of our knowledge, this is the first report of a true multivariate crystalline supramolecular alloy based on POCs.[19] The introduction of electron-deficient and therefore highly reactive aldehydes in any given ratio increases the stability and crystallinity of the obtained material in a step-wise fashion, without influencing the overall crystal packing. A formation study using different feed ratios suggests a faster reaction of fluorinated aldehydes in comparison to the non-fluorinated counterparts, where imine cage $\mathbf{A_4H_6}$ is formed slower. The fine tuning of the cavity of an organic cage will enable precise control over the selectivity of the resulting solid state materials in the future and marks an entry point for fluorinated organic cages into the field of supramolecular materials chemistry. Our study is an important addition to the dynamic covalent chemistry of complex POCs, employing three or more building blocks and lays the foundation for further research regarding exciting properties of this new class of organic cages.

© 2021 The Authors. Published by Wiley-VCH GmbH

Acknowledgements

We thank Dr. Markus Leutzsch of the MPI for Coal Research for help with the NMR measurements and Dr. Raphael Wiedey and Prof. Dr. Peter Kleinebudde for access to a powder X-ray diffractometer. This work was supported by the Fonds der Chemischen Industrie by a Kekulé Fellowship (T.K.) by the North Rhine-Westphalian Academy of Sciences, Humanities and the Arts (B.M.S.) and funded by the Deutsche Forschungs-gemeinschaft (DFG, German Research Foundation) – SCHM 3101/5-1. Open access funding enabled and organized by Projekt DEAL.

Conflict of Interest

The authors declare no conflict of interest.

Keywords: cage compounds · crystal structures · dynamic covalent chemistry · fluorine chemistry · materials

[1] a) A. G. Slater, A. I. Cooper, *Science* **2015**, *348*, aaa8075; b) T. Hasell, A. I. Cooper, *Nat. Rev. Mater.* **2016**, *1*, 16053.

[2] a) A. Cadiau, Y. Belmabkhout, K. Adil, P. M. Bhatt, R. S. Pillai, A. Shkurenko, C. Martineau-Corcos, G. Maurin, M. Eddaoudi, *Science* **2017**, *356*, 731–735; b) T.-H. Chen, I. Popov, O. Zenasni, O. Daugulis, O. Š. Miljanić, *Chem. Commun.* **2013**, *49*, 6846–6848; c) P. Pachfule, Y. Chen, J. Jiang, R. Banerjee, *Chem. Eur. J.* **2012**, *18*, 688–694; a recent review:; d) Z. Zhang, O. Š. Miljanić, *Org. Mat.* **2019**, *1*, 19–29.

[3] a) C. Yang, X. Wang, M. A. Omary, *J. Am. Chem. Soc.* **2007**, *129*, 15454–15455; b) C. Yang, U. Kaipa, Q. Z. Mather, X. Wang, V. Nesterov, A. F. Venero, M. A. Omary, *J. Am. Chem. Soc.* **2011**, *133*, 18094–18097; for recent reviews on fluorinated MOFs, see:; c) K. Jayaramulu, F. Geyer, A. Schneemann, Š. Kment, M. Otyepka, R. Zboril, D. Vollmer, R. A. Fischer, *Adv. Mater.* **2019**, *31*, 1900820; d) S.-I. Noro, T. Nakamura, *NPG Asia Mater.* **2017**, *9*, e433.

[4] a) P. M. Bhatt, Y. Belmabkhout, A. Cadiau, K. Adil, O. Shekhah, A. Shkurenko, L. J. Barbour, M. Eddaoudi, *J. Am. Chem. Soc.* **2016**, *138*, 9301–9307; b) T.-H. Chen, I. Popov, W. Kaveevivitchai, Y.-C. Chuang, Y.-S. Chen, A. J. Jacobson, O. Š. Miljanić, *Angew. Chem. Int. Ed.* **2015**, *54*, 13902–13906; *Angew. Chem.* **2015**, *127*, 14108–14112.

[5] a) A. Comotti, F. Castiglioni, S. Bracco, J. Perego, A. Pedrini, M. Negroni, P. Sozzani, *Chem. Commun.* **2019**, *55*, 8999–9002; b) G. Wang, K. Leus, H. S. Jena, C. Krishnaraj, S. Zhao, H. Depauw, N. Tahir, Y.-Y. Liu, P. Van Der Voort, *J. Mater. Chem. A* **2018**, *6*, 6370–6375; c) S. B. Alahakoon, G. T. McCandless, A. A. K. Karunathilake, C. M. Thompson, R. A. Smaldone, *Chem. Eur. J.* **2017**, *23*, 4255–4259.

[6] a) T.-H. Chen, I. Popov, W. Kaveevivitchai, Y.-C. Chuang, Y.-S. Chen, O. Daugulis, A. J. Jacobson, O. Š. Miljanić, *Nat. Commun.* **2014**, *5*, 5131; b) Z. Yang, S. Wang, Z. Zhang, W. Guo, K. Jie, M. I. Hashim, O. Š. Miljanić, D.-E. Jiang, I. Popovs, S. Dai, *J. Mater. Chem. A* **2019**, *7*, 17277–17282; c) T.-H. Chen, W. Kaveevivitchai, A. J. Jacobson, O. Š. Miljanić, *Chem. Commun.* **2015**, *51*, 14096–14098.

[7] a) M. I. Hashim, H. T. M. Le, T.-H. Chen, Y.-S. Chen, O. Daugulis, C.-W. Hsu, A. J. Jacobson, W. Kaveevivitchai, X. Liang, T. Makarenko, O. Š. Miljanić, I. Popovs, H. V. Tran, X. Wang, C.-H. Wu, J. I. Wu, *J. Am. Chem. Soc.* **2018**, *140*, 6014–6026; b) J.-H. Dou, Y.-Q. Zheng, Z.-F. Yao, Z.-A. Yu, T. Lei, X. Shen, X.-Y. Luo, J. Sun, S.-D. Zhang, Y.-F. Ding, G. Han, Y. Yi, J.-Y. Wang, J. Pei, *J. Am. Chem. Soc.* **2015**, *137*, 15947–15956; c) K. Reichenbächer, H. I. Süss, J. Hulliger, *Chem. Soc. Rev.* **2005**, *34*, 22–30.

[8] a) A. W. Markwell-Heys, M. L. Schneider, J. M. L. Madridejos, G. F. Metha, W. M. Bloch, *Chem. Commun.* **2021**, *57*, 2915–2918; b) R. A. S. Vasdev, J. A. Findlay, D. R. Turner, J. D. Crowley, *Chem. Asian J.* **2021**, *16*, 39–43; c) L. S. Lisboa, J. A. Findlay, L. J. Wright, C. G. Hartinger, J. D. Crowley, *Angew. Chem. Int. Ed.* **2020**, *59*, 11101–11107; *Angew. Chem.* **2020**, *132*, 11194–11200; d) M. L. Schneider, O. M. Linder-Patton, W. M. Bloch, *Chem. Commun.* **2020**, *56*, 12969–12972; e) D. Preston, A. R. Inglis, J. D. Crowley, P. E. Kruger, *Chem. Asian J.* **2019**, *14*, 3404–3408; f) S. Klotzbach, F. Beuerle, *Angew. Chem. Int. Ed.* **2015**, *54*, 10356–10360; *Angew. Chem.* **2015**, *127*, 10497–10502; g) A. Dhara, F. Beuerle, *Chem. Eur. J.* **2015**, *21*, 17391–17396; h) Kołodziejski, A. R. Stefankiewicz, J.-M. Lehn, *Chem. Sci.* **2019**, *10*, 1836–1843; for a review see:; i) F. Beuerle, B. Gole, *Angew. Chem. Int. Ed.* **2018**, *57*, 4850–4878; *Angew. Chem.* **2018**, *130*, 4942–4972; for nomenclature based on the topicity of the precursors as used herein, see; j) V. Santolini, M. Miklitz, E. Berardo, K. E. Jelfs, *Nanoscale* **2017**, *9*, 5280–5298.

[9] a) T. Tozawa, J. T. A. Jones, S. I. Swamy, S. Jiang, D. J. Adams, S. Shakespeare, R. Clowes, D. Bradshaw, T. Hasell, S. Y. Chong, C. Tang, S. Thompson, J. Parker, A. Trewin, J. Bacsa, A. M. Z. Slawin, A. Steiner, A. I. Cooper, *Nat. Mater.* **2009**, *8*, 973–978; b) V. Abet, F. T. Szczypiński, M. A. Little, V. Santolini, C. D. Jones, R. Evans, C. Wilson, X. Wu, M. F. Thorne, M. J. Bennison, P. Cui, A. I. Cooper, K. E. Jelfs, A. G. Slater, *Angew. Chem. Int. Ed.* **2020**, *59*, 16755–16763; *Angew. Chem.* **2020**, *132*, 16898–16906; c) M. Liu, L. Zhang, M. A. Little, V. Kapil, M. Ceriotti, S. Yang, L. Ding, D. L. Holden, R. Balderas-Xicohténcatl, D. He, R. Clowes, S. Y. Chong, G. Schütz, L. Chen, M. Hirscher, A. I. Cooper, *Science* **2019**, *366*, 613–620; d) R. L. Greenaway, V. Santolini, M. J. Bennison, B. M. Alston, C. J. Pugh, M. A. Little, M. Miklitz, E. G. B. Eden-Rump, R. Clowes, A. Shakil, H. J. Cuthbertson, H. Armstrong, M. E. Briggs, K. E. Jelfs, A. I. Cooper, *Nat. Commun.* **2018**, *9*, 2849; e) S. Jiang, Y. Du, M. Marcello, E. W. Corcoran Jr, D. C. Calabro, S. Y. Chong, L. Chen, R. Clowes, T. Hasell, A. I. Cooper, *Angew. Chem. Int. Ed.* **2018**, *57*, 11228–11232; *Angew. Chem.* **2018**, *130*, 11398–11402; f) M. J. Bojdys, M. E. Briggs, J. T. A. Jones, D. J. Adams, S. Y. Chong, M. Schmidtmann, A. I. Cooper, *J. Am. Chem. Soc.* **2011**, *133*, 16566–16571.

[10] a) J. C. Lauer, W.-S. Zhang, F. Rominger, R. R. Schröder, M. Mastalerz, *Chem. Eur. J.* **2018**, *24*, 1816–1820; b) S. M. Elbert, N. I. Regenauer, D. Schindler, W. S. Zhang, F. Rominger, R. R. Schröder, M. Mastalerz, *Chem. Eur. J.* **2018**, *24*, 11438–11443; c) D. Beaudoin, F. Rominger, M. Mastalerz, *Angew. Chem. Int. Ed.* **2017**, *56*, 1244–1248; *Angew. Chem.* **2017**, *129*, 1264–1268; d) M. W. Schneider, I. M. Oppel, A. Griffin, M. Mastalerz, *Angew. Chem. Int. Ed.* **2013**, *52*, 3611–3615; *Angew. Chem.* **2013**, *125*, 3699–3704; e) M. W. Schneider, I. M. Oppel, M. Mastalerz, *Chem. Eur. J.* **2012**, *18*, 4156–4160; for reviews about the topic see also:; f) M. Mastalerz, *Acc. Chem. Res.* **2018**, *51*, 2411–2422; g) M. Mastalerz, *Angew. Chem. Int. Ed.* **2010**, *49*, 5042–5053; *Angew. Chem.* **2010**, *122*, 5164–5175.

[11] a) T. Jiao, L. Chen, D. Yang, X. Li, G. Wu, P. Zeng, A. Zhou, Q. Yin, Y. Pan, B. Wu, X. Hong, X. Kong, V. M. Lynch, J. L. Sessler, H. Li, *Angew. Chem. Int. Ed.* **2017**, *56*, 14545–14550; *Angew. Chem.* **2017**, *129*, 14737–1474; b) T. Kunde, T. Pausch, G. R. Reiss, B. M. Schmidt, *Synlett* **2021**, https://doi.org/10.1055/a-1470–6050.

[12] a) Q. Liao, C. Ke, X. Huang, G. Zhang, Q. Zhang, Z. Zhang, Y. Zhang, Y. Liu, F. Ning, K. Xi, *J. Mater. Chem. A* **2019**, *7*, 18959–18970; b) B. M. Schmidt, A. K. Meyer, D. Lentz, *CrystEngComm.* **2017**, *19*, 1328–1333.

[13] T. Kunde, E. Nieland, H. V. Schröder, C. A. Schalley, B. M. Schmidt, *Chem. Commun.* **2020**, *56*, 4761–4764.

[14] S. Jiang, J. T. A. Jones, T. Hasell, C. E. Blythe, D. J. Adams, A. Trewin, A. I. Cooper, *Nat. Commun.* **2011**, *2*, 207.

[15] A. Simonov, A. L. Goodwin, *Nat. Chem. Rev.* **2020**, *4*, 657–673.

[16] T. H. Schick, F. Rominger, M. Mastalerz, *J. Org. Chem.* **2020**, *85*, 13757–13771.

[17] Deposition numbers 2047255 (for $\mathbf{A_4F_6}$), 2047256 ($\mathbf{A_4H_1F_5}$) and 2047257 ($\mathbf{A_4H_2F_4}$) contain the supplementary crystallographic data for this paper. These data are provided free of charge by the joint Cambridge Crystallographic Data Centre and Fachinformationszentrum Karlsruhe Access Structures service.

[18] H. Deng, C. J. Doonan, H. Furukawa, R. B. Ferreira, J. Towne, C. B. Knobler, B. Wang, O. M. Yaghi, *Science* **2010**, *327*, 846–850.

[19] a) A. G. Slater, M. A. Little, A. Pulido, S. Y. Chong, D. Holden, L. Chen, C. Morgan, X. Wu, G. Cheng, R. Clowes, M. E. Briggs, T. Hasell, K. E. Jelfs, G. M. Day, A. I. Cooper, *Nat. Chem.* **2017**, *9*, 17–25; b) M. A. Little, M. E. Briggs, J. T. A. Jones, M. Schmidtmann, T. Hasell, S. Y. Chong, K. E. Jelfs, L. Chen, A. I. Cooper, *Nat. Chem.* **2015**, *7*, 153–159; c) T. Hasell, S. Y. Chong, M. Schmidtmann, D. J. Adams, A. I. Cooper, *Angew. Chem. Int. Ed.* **2012**, *51*, 7154–7157; *Angew. Chem.* **2012**, *124*; 7266–7269.

Manuscript received: March 10, 2021
Accepted manuscript online: April 14, 2021
Version of record online: May 14, 2021

 © 2021 The Authors. Published by Wiley-VCH GmbH